Brain Stimulation xxx (2012) 1–7

Contents lists available at SciVerse ScienceDirect

Brain Stimulation

journal homepage: www.brainstimjrnl.com

Original Research

Stimulus intensity for hand held and robotic transcranial magnetic stimulation

Lars Richter [a,b,*], Peter Trillenberg [c], Achim Schweikard [a], Alexander Schlaefer [a,b,d]

[a] *Institute for Robotics and Cognitive Systems, University of Lübeck, 23562 Lübeck, Germany*
[b] *Graduate School for Computing in Medicine and Life Sciences, University of Lübeck, 23562 Lübeck, Germany*
[c] *Department of Neurology, University Hospital of Schleswig-Holstein, 23538 Lübeck, Germany*
[d] *Medical Robotics Group, University of Lübeck, 23562 Lübeck, Germany*

ARTICLE INFO

Article history:
Received 20 March 2012
Received in revised form
1 June 2012
Accepted 3 June 2012
Available online xxx

Key words:
Transcranial magnetic stimulation
Induced electric field
Motion compensation
Robotized TMS
Head rest

ABSTRACT

Background: Transcranial Magnetic Stimulation (TMS) is based on a changing magnetic field inducing an electric field in the brain. Conventionally, the TMS coil is mounted to a static holder and the subject is asked to avoid head motion. Additionally, head resting frames have been used. In contrast, our robotized TMS system employs active motion compensation (MC) to maintain the correct coil position.
Objective/hypothesis: We study the effect of patient motion on TMS. In particular, we compare different coil positioning techniques with respect to the induced electric field.
Methods: We recorded head motion for six subjects in three scenarios: (a) avoiding head motion, (b) using a head rest, and (c) moving the head freely. Subsequently, the motion traces were replayed using a second robot to move a sensor to measure the electric field in the target region. These head movements were combined with 2 types of coil positioning: (1) using a coil holder and (2) using robotized TMS with MC.
Results: After 30 min the induced electric field was reduced by 32.0% and 19.7% for scenarios (1a) and (1b), respectively. For scenarios (2a)–(2c) it was reduced by only 4.9%, 1.4% and 2.0%, respectively, which is a significant improvement ($P < 0.05$). Furthermore, the orientation of the induced field changed by 5.5°, 7.6°, 0.4°, 0.2°, 0.2° for scenarios (1a)–(2c).
Conclusion: While none of the scenarios required rigid head fixation, using a simple holder to position a coil during TMS can lead to substantial deviations in the induced electric field. In contrast, robotic motion compensation results in clinically acceptable positioning throughout treatment.

Introduction

Based on the principle of electromagnetic induction, Transcranial Magnetic Stimulation (TMS) is used for noninvasive stimulation of the brain [1]. Typically, a TMS coil is placed on the patient's head such that the maximum magnetic field covers the target region. Particularly, repetitive transcranial magnetic stimulation (rTMS) has become a promising tool for treatment of a variety of medication resistant neurological and psychiatric conditions. Clinical trials have proven effects, e.g., for depression [2], chronic tinnitus [3] or chronic pain [4]. Typically, rTMS is applied for 15–30 min for each single treatment session. Even more important is single-pulse TMS for brain research and cognitive neuroscience [5–7].

To locate the stimulation target and to position the coil, different approaches exist. In its simplest way, localization is based on external anatomical landmarks, e.g., midline or ear-to-ear-line. Another way is to take advantage of the 10–20 system of electrode placement for electroencephalogram (EEG) recordings [8]. The TMS coil can be placed relative to these electrode positions.

A recent technique for coil positioning and target localization is the application of neuro-navigation [9]. Neuro-navigation combines a three-dimensional (3D) scan of the patient's head with a realtime tracking system. After registration and with tracking of coil and head, the TMS coil can be positioned based on the 3D head scan. Hence, neuro-navigated TMS is the state-of-the-art tool for precise target localization [10,11].

As holding the coil by hand for a stimulation sequence of up to 30 min is an exhausting task, commonly a rigid holder or

This work was partially supported by the Graduate School for Computing in Medicine and Life Sciences funded by Germany's Excellence Initiative [DFG GSC 235/1]. All authors reported no biomedical financial interests or potential conflicts of interest.
* Corresponding author. Institute for Robotics and Cognitive Systems, University of Lübeck, Ratzeburger Allee 160, 23562 Lübeck, Germany. Tel.: +49 451 5005207; fax: +49 451 5005202.
E-mail address: richter@rob.uni-luebeck.de (L. Richter).

1935-861X/$ – see front matter
http://dx.doi.org/10.1016/j.brs.2012.06.002

mechanical arm retains the TMS coil after positioning [12]. This way, the coil maintains its position during stimulation. However, the stimulation point will not necessarily be stable over time as the patient's head may move. The easiest and often used solution is to ask the patient to keep the head as still as possible while maintaining contact to the coil. Another solution is using a head resting frame (chin rest) where the patient puts the chin in a mold and presses the forehead against a frame [12,13]. The aim of such a frame is additional head stabilization [14]. Obviously, a rigid head fixation, like in radiation therapy, would bring head motion to a minimum [15]. However, it cannot generally be used for TMS as it leads to serious discomfort for the patient and results in stress and excitement.

In contrast, robotized systems for TMS are advancing for exact targeting [11,16]. For robotized TMS, the magnetic coil is placed directly on the patient's head using a robot [17]. Continuous tracking of the head motion allows to compute the target position throughout treatment. As the shape of the head is known from 3D images, the robot positions the TMS coil automatically at the stimulation point in a tangential orientation to the cranium [18]. Once the target point is reached, motion compensation (MC) is activated. This compensates changes in the position of the stimulation point or orientation of the head with appropriate robot movements to keep high accuracy during treatment [19].

Measuring the accuracy of TMS in vivo is rather difficult. Only motor cortex stimulation results in a quantitatively detectable activity. Using surface electrodes motor evoked potentials (MEPs) can be measured for a target muscle. However, the variance in the MEP amplitude is quite large [20]. Hence, the accuracy of TMS in general cannot be derived from the MEP amplitude.

To study the impact of motion on TMS, and to evaluate the effectiveness of different approaches to handle motion, we investigate different scenarios to perform TMS. First, we propose to assess the end-to-end effect of motion based on measurement of the actual electric field. Second, we describe three different treatment scenarios and our setup to measure head motion. Third, we study a number of recorded motion traces and establish the actual effect on TMS by measuring the induced electric fields. Finally, we discuss our results, which indicate that active motion compensation using a robotized TMS system provides superior accuracy with respect to magnitude and orientation of the electric field.

Preliminary results of this study have been already presented as a conference abstract in [21].

Methods

Principle of end-to-end accuracy

In general, TMS is applied for cortical brain stimulation. The target region is therefore located approximately 2–5 cm beneath the TMS coil [22]. For an optimal stimulation the investigator aligns the coil tangentially to the cranium. Thus, the coil is approximately parallel to the cortex surface.

For TMS, the coil produces a rapidly changing magnetic field. The magnetic field passes through the skull and induces an electric field inside the cortex which leads to cortical stimulation [23,24]. A closer look at the magnetic field of a typical figure-of-eight coil reveals that the magnetic field B is virtually parallel to the coil's principal axis (z-axis) in the target range. In the target region we can therefore assume the induced electric field E being perpendicular to the coil's principal axis. Hence, we assume the z-directed induced electric field E_z to be zero [25]. Note that for circular coils the target region is circular beneath the full coil instead of below the coil's center for figure-of-eight coils. Nonetheless, the same principle is also valid for circular coils.

A slight tilt of the coil, however, will also lead the magnetic field to be slightly non-perpendicular to the cortex. Nevertheless, the primary component of stimulation will be parallel to the cortex surface. We therefore neglect the z-component of the electric field.

We use a field sensor embedded in a human head phantom that exactly corresponds to the stimulation process in the cortex. This sensor measures the induced electric field E in the cortex in the x/y-plane.

Besides the magnitude of the induced electric field, the orientation plays an important role for figure-of-eight coils [26–28]. It has been shown that the optimal current direction induced in the brain is almost perpendicular to the central sulcus [29,30]. With our setup, we can also measure the coil rotation about its z-axis.

To study the impact of motion on the stimulation accuracy, we record actual head motion during realistic TMS treatment scenarios. An optical tracking system records position and orientation of a marker integrated in a headband which a subject wears. The subject sits in front of a robotized TMS system and the marker is tracked. The tracking system is calibrated to the robot and therefore we can directly record marker and head motion in robot coordinates. This way, we record for each timestamp t a homogeneous 4×4 transformation matrix M. This matrix consists of a 3×3 rotational part, including the rotation angles, and a translational part representing the three-dimensional position.

As real head motion is now available in robot coordinates, we can mount the field sensor—embedded in the head phantom—to a robot *R1* to mimic the recorded head motion. The field sensor will exactly retrace the recorded head motion to simulate real TMS scenarios. For stimulation, we use a second robot *R2* placed next to the first robot *R1* and mount the TMS coil to *R2* (Fig. 1). We calibrate *R2* to the tracking system and attach a marker to the head phantom. We can now use the second robot to actively compensate for the residual head motion measured with the marker. While we replay the head motion, we measure the induced electric field produced by the TMS coil with the field sensor. Note that we move the head motion relative to a given starting position. Therefore, we must transfer the center of rotation from robot end effector to the marker, apply the relative rotation and transfer the center of rotation back to move the robot.

Realization & data acquisition

Head motion measurements

First, we recorded head motion for three different typical TMS scenarios:

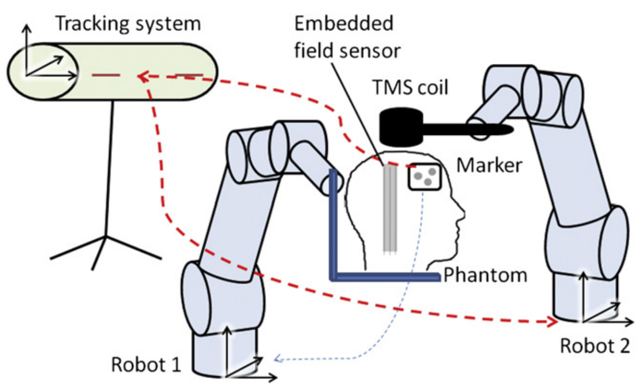

Figure 1. Schematic setup of motion replay. We use one robot with a field sensor, embedded in a head phantom, to replay the recorded head motion. A tracking system is calibrated to a second robot and tracks a marker attached to the head phantom. The second robot carries the TMS coil and compensates for head motion.

a) *restrain*: avoiding head motion,
b) *rest*: using a head rest, and
c) *freely*: moving the head freely.

For *restrain* the subject sits on a treatment chair and is asked to avoid head motion during recording. A coil holder (Magic Arm; Lino Manfrotto + Co. Spa, Bassano del Grappa, Italy) retains the coil after coil positioning on the head. An additional head resting frame helps the subject maintain its head pose in *rest*. For *freely* the coil is mounted to a robot (Viper s850; Adept Technology, Inc., Livermore, CA, USA) and motion is actively compensated by respective coil motion [19]. For this reason, head motion is not restricted.

A Polaris stereo-optic infrared tracking system (Northern Digital, Inc., Waterloo, Ontario, Canada) records the head motion by tracking a passive marker at the subjects' head. We calibrate the tracking system to the robot to store the head motion in robot coordinates [31]. For each scenario, we record head motion for 30 min. Six healthy subjects (aged 25–30 years) participated in the recording.

Note that the tracking system provides full 6 degrees-of-freedom for tracking the marker. Hence, we measure the rotational head motion in degrees besides the translational movement in mm.

Electric field measurements

For stimulus intensity measurements, we have designed a custom built sensor consisting of a plastic bar and two perpendicular wires (Fig. 2B). The plastic bar has a diameter of 10 mm and a length of 220 mm. The sensor is embedded in a styrofoam head phantom with dimensions similar to a human head (Fig. 2A). The sensor is located 15 mm below the outer head surface and at the head's midline (denoted with a red circle in Fig. 2D). Note that the styrofoam head is not necessary but allows to use the same setup as with actual patients. The sensor measures the induced electric field in the x/y-plane in the intersecting wires on top of the bar (Fig. 2C). Thus, the sensor uses two channels perpendicular to one another to detect the induced electric field in the *x*- and the *y*-axis simultaneously. This way, this sensor setup represents the cortical design in the brain, and is therefore sufficient for stimulus intensity measurements.

For motion replay, we use two identical Adept Viper s850 industrial robots combined with a Polaris tracking system. The tracking system is positioned opposite to the robots and calibrated to the second robot *R2* [31]. The first robot *R1* moves the head phantom incl. the field sensor according to the recorded head motion. *R2* holds and positions the TMS coil. Fig. 3 shows this setup.

R1 is moved to a starting position *S*. *R2* places the coil approximately 5 mm above the head phantom. Moreover the coil is aligned such that induced electric field in the target is maximal and the coil is in a tangential orientation with respect to the head surface. The first robot replays the recorded head movements relatively to *S*.

A standard MCF-B65 figure-of-eight coil connected to a MagPro X100 stimulator (MagVenture A/S, Farum, Denmark) generates the induced electric fields. The TMS stimulus strength is set to 50% of maximum stimulator output (MSO). A PC sends trigger pulses at about 1 Hz to the stimulator and reads the measured voltages induced in the sensor from a digital oscilloscope (Agilent Technologies, Inc., Santa Clara, CA, USA).

Typical TMS scenarios

We use the recorded head motion to measure stimulus intensity for distinct TMS scenarios. Therefore, we combine the head movements with 2 types of coil positioning: *hold* uses a static coil holder, and *robot* uses robotized TMS with active motion compensation. This way, we also investigate the impact of head motion restriction to the motion compensated TMS system, besides evaluation of the recorded scenarios:

1. *Hold-and-restrain*: Coil holder and avoiding head motion,
2. *Hold-and-rest*: Coil holder and a head rest,
3. *Robot-freely*: Robotized TMS with motion compensation (MC),
4. *Robot-and-restrain*: Robotized TMS with MC and avoiding head motion, and
5. *Robot-and-rest*: Robotized TMS with MC in combination with a head rest.

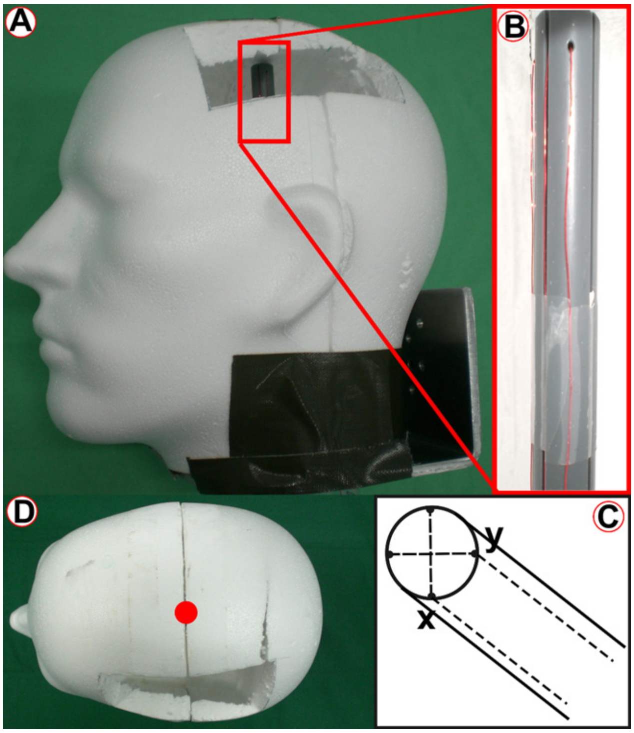

Figure 2. (A) The field sensor is integrated in a head phantom made of styrofoam and located 15 mm below the outer head surface. (B) The sensor consists of a plastic bar (diameter: 10 mm, length: 220 mm) with wires. (C) The sensor measures the induced electric field in the *x*/*y*-plane using two perpendicular wires (*x* and *y*, in dotted lines) on top of the sensor. The connections of the wires descend vertically and thus, they are not influenced by the electric field. (D) Top view of the head phantom (*x*/*y*-plane). The sensor's location is marked with a red circle. (For interpretation of the references to colour in this figure legend, the reader is referred to the web version of this article.)

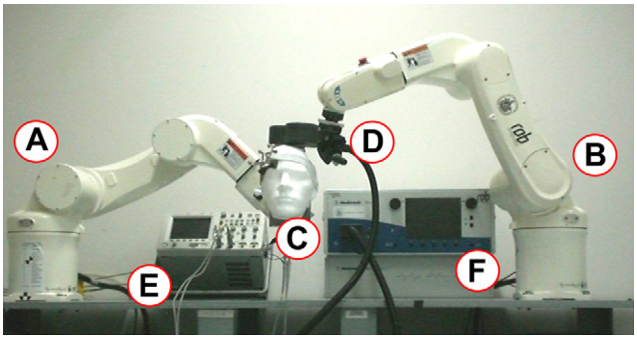

Figure 3. Setup of the movement retrace based on two identical industrial robots: The first robot (A) replays the recorded head motion holding a head phantom (C) and the second robot (B) carries the TMS coil (D) for the robotized TMS application. An Oscilloscope (E) measures the induced electric field and the TMS coil is connected to a TMS stimulator (F).

To this end, we replay head motion from *restrain* for *hold-and-restrain* and *robot-and-restrain*. For *hold-and-rest* and *robot-and-rest* we use head motion from *rest* and we replay head motion from *freely* for *robot-freely*. Note that we cannot combine *hold* with *freely* for measurement, as the head motion in *freely* is too large for a static positioning scenario.

Error calculation

We cannot assume that the sensor to coil distance or the sensor position are exactly the same for each single measurement. As this may change the absolute induced electric field magnitude, we cannot apply an absolute error measure. Instead, we calculate the decrease in the magnitude of the induced electric field as a relative error measure. At each timestamp t we compute the error relative to the initial field. The change in magnitude is defined as:

$$\mathrm{err}_{\mathrm{rel}}(t) = \left|1 - \|E(t)\|/\|E(0)\|\right|, \ \mathrm{err}_{\mathrm{rel}}(t) \in [0;1]$$

where $\|\cdot\|$ represents the Euclidean norm.

Our field sensor additionally measures the in-plane orientation of the electric field. We obtain the change in the angle as:

$$\sigma(t) = \left|\arctan(E_y(0)/E_x(0)) - \arctan(E_y(t)/E_x(t))\right|$$

based on the x and y component of the electric field E.

Statistical analysis

Statistical analysis was carried out with IBM SPSS Statistics version 20 (IBM Deutschland GmbH, Ehningen, Germany).

As we are interested in the effect of robotized TMS compared to standard TMS scenarios, we perform an analysis of variance (ANOVA) comparing the means of *Hold-and-restrain*, *Hold-and-rest* and *Robot-freely* for statistical analysis. Note that a two-factorial ANOVA cannot be used as we cannot measure *freely* with a coil holder.

Results

Head motion

Fig. 4 visualizes the mean amplitude of translational and rotational head motion over time for all subjects. In the two subplots the three basic scenarios are shown. When comparing the amount of head motion, we see that for *freely* the amplitude is essentially largest. Interestingly, the head motion when using a coil holder and a head rest (*rest*) is only slightly less compared to using a coil holder and avoiding head motion (*restrain*).

The mean translational head motion is 13.7 mm, 11.6 mm and 47.9 mm with a mean rotational motion of 3.9°, 3.8° and 11.9° for *restrain*, *rest* and *freely*, respectively. The standard deviation (SD) for translational head motion is 8.1 mm, 11.0 mm and 37.5 mm, respectively, and for rotational head motion 2.6°, 2.7° and 8.4°, respectively. Additionally, the mean values and SDs at six different time points are summarized in Table 1 for changes in position and orientation.

End-to-end accuracy

On average, the induced electric field in the sensor has had an electric field strength of 77.5 V/m with a SD of 4.0 V/m at starting time of the measurements. Taking the stimulation intensity of 50% of MSO into account, the measured electric field strength is in the expected range and therefore suggests that the measurements have been performed correctly.

Fig. 5A illustrates the average decrease in the magnitude of the induced electric fields. After 30 min the mean induced electric field is 32.0% lower than the initial value for *hold-and-restrain* and 19.7% lower for *hold-and-rest*. In contrast, the field is 4.9 %, 1.3 % and 1.9 % lower than the initial value for setups using the robotized TMS system: *robot-freely*, *robot-and-restrain* and *robot-and-rest*, respectively. The decrease for all measurement setups are summarized in Table 2 for six different time points. Additionally, the mean values and the standard deviations (SD) are given in the table. The improvement in accuracy of robotized TMS (*robot-freely*) compared to the two standard setups (*hold-and-restrain* and *hold-and-rest*) was significant ($P < 0.05$).

Fig. 5B visualizes the change in orientation of the induced electric fields over time averaging the measurements for all subjects. It is clearly visible that the error in orientation for the two common scenarios, *hold-and-restrain* and *hold-and-rest*, increases for the first 15 min and then remains almost constant. Surprisingly, the change for *hold-and-rest* is slightly larger compared to *hold-and-restrain*. In contrast, the change for the motion compensated setups stays constant at a very low level for the full duration.

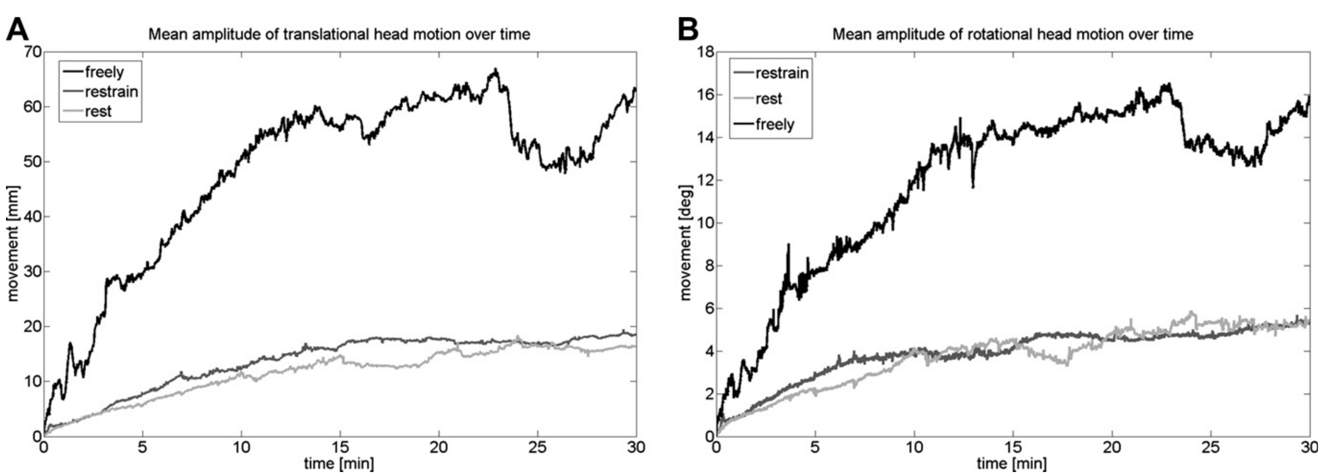

Figure 4. Mean amplitude of head motion over time for the different movement setups: Using the robotized system with motion compensation (black), using a coil holder and avoiding head motion (dark gray) and using a coil holder and a head rest (light grey). (A) shows the amplitude of translational head motion (in [mm]); (B) shows the amplitude of rotational head motion (in [°]).

Table 1
Mean magnitude with standard deviations (SD) of translational and rotational head motion for the three motion scenarios restrain, rest and freely at six different time points. Furthermore, overall means and SDs are displayed.

	5 min	10 min	15 min	20 min	25 min	30 min	Mean
Translational [mm]							
Restrain	7.7 ± 3.1	12.2 ± 5.6	16.4 ± 7.8	17.7 ± 8.6	17.0 ± 8.2	18.5 ± 8.7	13.7 ± 8.1
Rest	5.7 ± 5.5	11.4 ± 8.5	14.8 ± 10.2	15.3 ± 12.1	16.3 ± 15.0	16.4 ± 15.1	11.6 ± 11.0
Freely	29.5 ± 28.0	50.5 ± 39.6	56.1 ± 50.1	62.0 ± 48.7	52.6 ± 20.0	62.7 ± 22.2	47.9 ± 37.5
Rotational [°]							
Restrain	2.8 ± 1.9	3.9 ± 1.8	4.1 ± 2.7	4.5 ± 2.8	4.8 ± 3.2	5.3 ± 3.4	3.9 ± 2.6
Rest	2.2 ± 1.4	4.0 ± 2.2	4.6 ± 2.2	4.8 ± 2.6	5.3 ± 3.5	5.4 ± 3.7	3.8 ± 2.7
Freely	7.7 ± 5.6	11.9 ± 7.9	13.9 ± 11.6	15.2 ± 10.1	13.7 ± 5.8	15.8 ± 5.9	11.9 ± 8.4

After 30 min, the orientation has changed 5.5° for *hold-and-restrain* and 7.6° for *hold-and-rest*. The change in orientation is 0.4°, 0.2° and 0.2°, respectively, for the motion compensated scenarios. Table 2 additionally summarizes the change in orientation for six time points with the mean values and SDs for all measurement scenarios.

Discussion

Even though the magnitude of head motion over time is relatively small, less than 20 mm and less than 6° after 30 min, the impact on the induced electric field is very strong when using *hold-and-restrain* or *hold-and-rest*. After 10 min the intensity of the induced electric field in the cortex is 14–18% lower than the initial value. After 30 min this is even worse when head motion results in a reduction of the field magnitude of 32% and 20%, respectively. Besides a decrease in the induced electric field strength, the orientation of the field changed up to 8.6° and 10.6°, respectively.

Note that the change in electric field orientation is larger than the actual head rotation. Due to the translational head motion, the target point moves from the center of the coil. As the coil's electric field is composed from two ringlike electric fields [25], a shift of the target point also results in a change of the electric field direction. As there is an optimal direction of induced currents in the brain [29,30], a stable orientation is of crucial importance for comparable stimulation outcomes.

The robotized TMS system has a latency of approximately 200–300 ms and therefore cannot follow head movements instantaneously [19]. For continuous motion, this latency would be problematic [32,33]. In this case, we can expect a constant error. For TMS, however, only spontaneous motion is likely as supported by the recorded head motion. Our results for the robotized scenarios indicate that the effect of the system latency can be neglected for TMS. On average, the electric field intensity decreases <4% due to mispositioning. Also, the orientation of the induced electric field maintains constant (<0.5°). More interestingly, this is also true when head motion is not restricted (*move-freely*). Thus, usage of a head rest or asking the patient to not move the head is not required for the robotized system to maintain stimulation accuracy. *Robot-and-restrain* and *robot-and-rest* lead only to a very slight further improvement in stimulation accuracy.

The recorded head motions in our study were taken from young, healthy and cooperative volunteers. This may be a reason for the relative small movements. For patients suffering from neurological or psychiatric diseases, however, we can expect larger head movements. In this case, the influence on the induced electric field and therefore on the stimulation outcome might be even worse for *hold-and-restrain* and *hold-and-rest*. For the robotic TMS system, in contrast, the results indicate that active motion compensation will also be capable for larger head movements.

For TMS, as a focal brain stimulation technique, target identification is essential [11]. In recent years much effort was made to find optimal stimulation parameters for best stimulation outcomes when using repetitive TMS (rTMS) for different neurological or psychiatric conditions. As an example, recent studies used positron-emission tomography (PET) [34,35] or functional magnetic resonance imaging (fMRI) [36] to detect the stimulation target in the primary auditory cortex (PAC) for the treatment of chronic tinnitus. Furthermore, various studies were conducted using different frequency or stimulation intensity settings. Also, the stimulation duration and the number of total stimulation pulses differed [11,36,37].

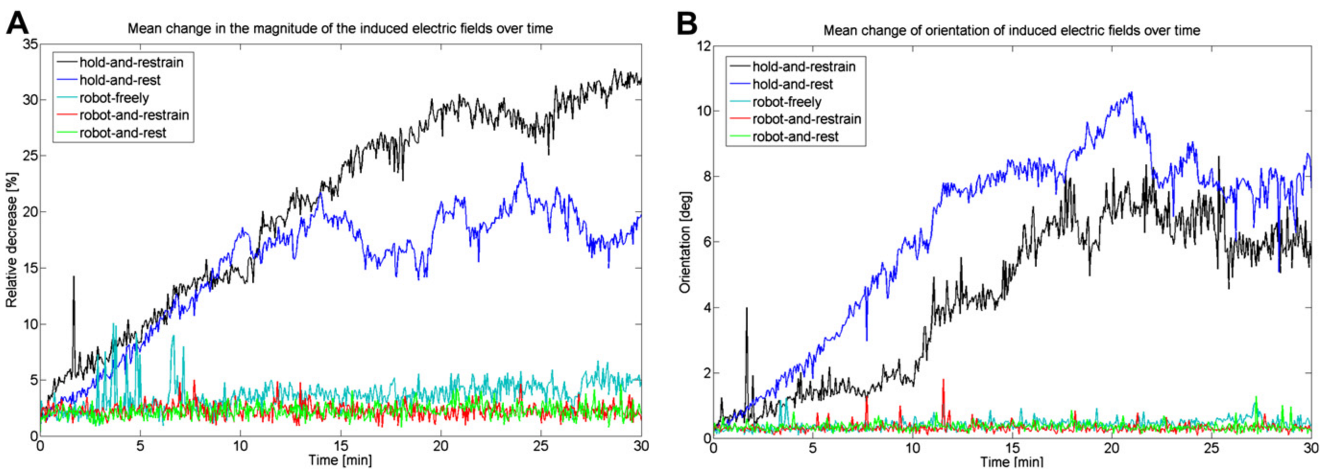

Figure 5. Change of the induced electric fields over time. (A) Mean decrease of the induced electric field magnitude relative to the starting point (in [%]). (B) Mean orientation change (in [°]).

Table 2
Mean decrease of induced electric field magnitude and orientation change with SD at six different time points. Furthermore, overall means and SDs are displayed.

	5 min	10 min	15 min	20 min	25 min	30 min	Mean
Magnitude decrease [%]							
Hold-and-restrain	8.4 ± 7.3	14.1 ± 11.8	23.1 ± 13.5	29.2 ± 13.8	27.6 ± 14.7	32.0 ± 14.9	20.6 ± 14.6
Hold-and-rest	8.0 ± 10.1	17.7 ± 17.4	18.9 ± 15.1	20.9 ± 15.1	20.6 ± 13.7	19.7 ± 13.8	15.1 ± 13.6
Robot-freely	2.2 ± 2.4	4.4 ± 2.9	2.0 ± 1.1	3.9 ± 3.2	4.8 ± 2.7	4.9 ± 1.9	3.7 ± 3.2
Robot-and-restrain	2.1 ± 0.6	1.8 ± 1.8	2.6 ± 1.5	2.6 ± 1.7	1.2 ± 1.1	1.4 ± 1.3	2.2 ± 1.6
Robot-and-rest	3.0 ± 2.2	2.4 ± 1.7	1.7 ± 0.9	2.4 ± 2.3	2.3 ± 1.0	2.0 ± 1.3	2.2 ± 1.6
Orientation change [°]							
Hold-and-restrain	1.5 ± 1.0	1.6 ± 1.1	5.3 ± 5.3	6.5 ± 6.5	6.9 ± 7.2	5.5 ± 6.4	4.3 ± 5.3
Hold-and-rest	2.6 ± 4.0	5.9 ± 10.9	8.4 ± 15.5	10.0 ± 18.8	8.2 ± 14.2	7.6 ± 12.0	6.3 ± 11.9
Robot-freely	0.4 ± 0.2	0.3 ± 0.2	0.3 ± 0.1	0.4 ± 0.2	0.5 ± 0.4	0.4 ± 0.4	0.4 ± 0.4
Robot-and-restrain	0.3 ± 0.3	0.3 ± 0.2	0.5 ± 0.3	0.3 ± 0.2	0.3 ± 0.3	0.2 ± 0.4	0.3 ± 0.4
Robot-and-rest	0.3 ± 0.3	0.2 ± 0.1	0.6 ± 0.5	0.4 ± 0.4	0.3 ± 0.3	0.2 ± 0.2	0.3 ± 0.3

For targeting the PAC, the cortical target region is relatively small. On average, its cortical length and width are 9.8 mm and 6.0 mm, respectively, [38]. When using a coil holder with motion avoidance or with a head rest for rTMS (*move-and-restrain* and *move-and-rest*), after 10 min the total translational head movement can be >10 mm. Hence, the stimulation focus will move out of PAC and the selected cortical target region will only be stimulated partially. Most of the induced electric field will be delivered to a neighboring brain region. Therefore, after 10 min of stimulation, the stimulation will not be as effective as in the beginning. Note that the target region also has roughly the same size for most other TMS applications.

However, increasing the stimulation intensity by 20% or 30% to compensate for the decrease of the induced electric field in the target to reach the desired electric field strength is no solution. Although this would yield the planned stimulation strength in the target, there will be one other cortical region that will be exposed to 120% or 130% of the stimulation intensity as it is now in the coil's focus. This can lead to undesired effects and is potentially dangerous [39].

In contrast, the robotized TMS system with active motion compensation maintains the stimulation strength and orientation in the target region as planned. Hence, advanced navigated treatments based on image planning location and direction can be delivered.

Conclusion

Head motion occurs during TMS applications and cannot be suppressed completely. Even small changes in the position and/or orientation of the coil with respect to the target can have a substantial impact on the stimulus intensity and therefore on the stimulation outcome. Robotic motion compensation, however, effectively offsets these changes, thus maintaining the initial magnitude and orientation throughout treatment.

In conclusion, the robotized TMS system is an important tool for successful treatments and investigations using (repetitive) Transcranial Magnetic Stimulation.

References

[1] Barker AT, Jalinous R, Freeston IL. Non-invasive magnetic stimulation of human motor cortex. Lancet 1985 May;1(8437):1106–7.
[2] Fitzgerald PB, Hoy K, McQueen S, Maller JJ, Herring S, Segrave R, et al. A randomized trial of rTMS targeted with MRI based neuro-navigation in treatment-resistant depression. Neuropsychopharmacology 2009 Jan;34(5): 1255–62.
[3] Kleinjung T, Eichhammer P, Langguth B, Jacob P, Marienhagen J, Hajak G, et al. Long-term effects of repetitive transcranial magnetic stimulation (rTMS) in patients with chronic tinnitus. Otolaryngology - Head and Neck Surgery 2005; 132(4):566–9.
[4] Mhalla A, Baudic S, de Andrade DC, Gautron M, Perrot S, Teixeira MJ, et al. Long-term maintenance of the analgesic effects of transcranial magnetic stimulation in fibromyalgia. Pain 2011;152(7):1478–85.
[5] Pascual-Leone A, Walsh V, Rothwell JC. Transcranial magnetic stimulation in cognitive neuroscience — virtual lesion, chronometry, and functional connectivity. Current Opinion in Neurobiology 2000;10:232–7.
[6] Ziemann Ulf. TMS in cognitive neuroscience: virtual lesion and beyond. Cortex 2010;46(1):124–7.
[7] Sandrini M, Umilt`a C, Rusconi E. The use of transcranial magnetic stimulation in cognitive neuroscience: a new synthesis of methodological issues. Neuroscience & Biobehavioral Reviews 2011;35(3):516–36.
[8] Jasper HH. The ten-twenty electrode system of the international federation. Electroencephalography and Clinical Neurophysiology 1958;10(2):371–5.
[9] Ruohonen J, Karhu J. Navigated transcranial magnetic stimulation. Neurophysiologie Clinique/Clinical Neurophysiology 2010;40(1):7–17.
[10] Siebner HR, Bergmann TO, Bestmann S, Massimini M, Johansen-Berg H, Mochizuki H, et al. Consensus paper: combining transcranial stimulation with neuroimaging. Brain Stimulation 2009;2(2):58–80.
[11] Langguth B, Kleinjung T, Landgrebe M, Ridder DD, Hajak G. rTMS for the treatment of tinnitus: the role of neuronavigation for coil positioning. Neurophysiologie Clinique/Clinical Neurophysiology 2010 March;40(1):45–58.
[12] Chronicle EP, Pearson AJ, Matthews C. Development and positioning reliability of a TMS coil holder for headache research. Headache: The Journal of Head and Face Pain 2005;45(1):37–41.
[13] Reichenbach A, Whittingstall K, Thielscher A. Effects of transcranial magnetic stimulation on visual evoked potentials in a visual suppression task. NeuroImage 2011;54(2):1375–84.
[14] Sprenger A, Trillenberg P, Pohlmann J, Herold K, Lencer R, Helmchen C. The role of prediction and anticipation on age-related effects on smooth pursuit eye movements. Annals of the New York Academy Sciences 2011;1233:168–76.
[15] Weltens C, Kesteloot K, Vandevelde G, den Bogaert WV. Comparison of plastic and orfit masks for patient head fixation during radiotherapy: precision and costs. International Journal of Radiation Oncology, Biology, Physics 1995; 33(2):499–507.
[16] Kantelhardt S, Fadini T, Finke M, Kallenberg K, Bockermann V, Matthäus L, et al. Robotized image-guided transcranial magnetic stimulation, a novel technique for functional brain-mapping. Clinical Neurophysiology 2009 Jan; 120(1):e84.
[17] Matthäus L. A robotic assistance system for transcranial magnetic stimulation and its application to motor cortex mapping. Universität zu Lübeck; 2008.
[18] Matthäus L, Giese A, Wertheimer D, Schweikard A. Planning and analyzing robotized TMS using virtual reality. Studies in Health Technology Informatics 2006;119:373–8.
[19] Richter L, Matthäus L, Schlaefer A, Schweikard A. Fast robotic compensation of spontaneous head motion during transcranial magnetic stimulation (TMS). In: UKACC international conference on CONTROL 2010, 8. Coventry, UK: United Kingdom Automatic Control Council; 2010. p. 872–7.
[20] Zarkowski P, Shin CJ, Dang T, Russo J, Avery D. EEG and the variance of motor evoked potential amplitude. Clinical EEG & Neuroscience 2006 Jul;(3):247–51.
[21] Richter L, Trillenberg P, Schweikard A, Schlaefer A. Comparison of stimulus intensity in hand held and robotized motion compensated transcranial magnetic stimulation. Neurophysiologie Clinique/Clinical Neurophysiology 2012 Jan;42(1–2):61–2 [Abstracts of the 2012 Burgundy Meeting].
[22] Stokes MG, Chambers CD, Gould IC, English T, McNaught E, McDonald O, et al. Distance-adjusted motor threshold for transcranial magnetic stimulation. Clinical Neurophysiology 2007;118(7):1617–25.
[23] Ruohonen J, Ilmoniemi RJ. Modeling of the stimulating field generation in TMS. Electroencephalography and Clinical Neurophysiology Supplements 1999;51:30–40.
[24] Ruohonen J. Transcranial magnetic stimulation: modelling and new techniques [dissertation]. Helsinki University of Technology, Laboratory of Biomedical Engineering (BioMag); 1998.
[25] Salinas FS, Lancaster JL, Fox PT. Detailed 3D models of the induced electric field of transcranial magnetic stimulation coils. Physics in Medicine and Biology 2007 May;52(10):2879–92.

[26] Balslev D, Braet W, McAllister C, Miall RC. Interindividual variability in optimal current direction for transcranial magnetic stimulation of the motor cortex. Journal of Neuroscience Methods 2007;162(1–2):309–13.
[27] Pascual-Leone A, Cohen LG, Brasil-Neto JP, Hallett M. Noninvasive differentiation of motor cortical representation of hand muscles by mapping of optimal current directions. Electroencephalography and clinical Neurophysiology 1994;93:42–8.
[28] Werhahn KJ, Fong JKY, Meyer BU, Priori A, Rothwell JC, Day BL, et al. The effect of magnetic coil orientation on the latency of surface EMG and single motor unit responses in the first dorsal interosseous muscle. Electroencephalography and clinical Neurophysiology 1994;93:138–46.
[29] Brasil-Neto JP, Cohen LG, Panizza M, Nilsson J, Roth BJ, Hallett M. Optimal focal transcranial magnetic activation of the human motor cortex: effects of coil orientation, shape of the induced current pulse, and stimulus intensity. Journal of Clinical Neurophysiology 1992 Jan;9(1):132–6.
[30] Mills KR, Boniface SJ, Schubert M. Magnetic brain stimulation with a double coil: the importance of coil orientation. Electroencephalography and clinical Neurophysiology 1992;85:17–21.
[31] Ernst F, Richter L, Matthäus L, Martens V, Bruder R, Schlaefer A, et al. Non-orthogonal tool/flange and robot/world calibration for realistic tracking scenarios. The International Journal of Medical Robotics and Computer Assisted Surgery 2012 [accepted for publication].
[32] Fürweger C, Drexler C, Kufeld M, Muacevic A, Wowra B, Schlaefer A. Patient motion and targeting accuracy in robotic spinal radiosurgery: 260 single-fraction fiducial-free cases. International Journal of Radiation Oncology, Biology, Physics 2010;78(3):937–45.
[33] Murphy MJ, Chang SD, Gibbs IC, Le QT, Hai J, Kim D, et al. Patterns of patient movement during frameless image-guided radiosurgery. International Journal of Radiation Oncology, Biology, Physics 2003;55(5):1400–8.
[34] Plewnia C, Reimold M, Najib A, Brehm B, Reischl G, Plontke SK, et al. Dose-dependent attenuation of auditory phantom perception (Tinnitus) by PET-guided repetitive transcranial magnetic stimulation. Human Brain Mapping 2007;28:238–46.
[35] Plewnia C, Reimold M, Najib A, Reischl G, Plontke SK, Gerloff C. Moderate therapeutic efficacy of positron emission tomography-navigated repetitive transcranial magnetic stimulation for chronic tinnitus: a randomised, controlled pilot study. Journal of Neurology Neurosurgery and Psychiatry 2007;78:152–6.
[36] Londero A, Langguth B, Ridder DD, Bonfils P, Lefaucheur JP. Repetitive transcranial magnetic stimulation (rTMS): a new therapeutic approach in subjective tinnitus? Neurophysiologie Clinique/Clinical Neurophysiology 2006; 36(3):145–55.
[37] Langguth B, De Ridder D, Dornhoffer JL, Eichhammer P, Folmer RL, Frank E, et al. Controversy: does repetitive transcranial magnetic stimulation/transcranial direct current stimulation show efficacy in treating tinnitus patients? Brain Stimulation 2008;1:192–205.
[38] Artacho-Pérula E, Arbizu J, del Mar Arroyo-Jimenez M, Marcos P, Martinez-Marcos A, Blaizot X, et al. Quantitative estimation of the primary auditory cortex in human brains. Brain Research 2004;1008(1):20–8.
[39] Rossi S, Hallett M, Rossini PM, Pascual-Leone A. Safety, ethical considerations, and application guidelines for the use of transcranial magnetic stimulation in clinical practice and research. Clinical Neurophysiology 2009;120(12): 2008–39.